

Electroweak corrections to top quark pair production in association with a hard photon at hadron colliders

Peng-Fei Duan,¹ Yu Zhang *,^{2,1} Yong Wang,³ Mao Song,⁴ and Gang Li⁴

¹*City College, Kunming University of Science and Technology,
Kunming, Yunnan 650051, China*

²*School of Physics, Nanjing University,
Nanjing, Jiangsu, 210093, China*

³*Department of Modern Physics, University of Science and Technology of China,
Hefei, Anhui 230026, P.R.China*

⁴*School of Physics and Material Science, Anhui University,
Hefei, Anhui 230039, China*

Abstract

We present the next-to-leading order (NLO) electroweak (EW) corrections to the top quark pair production associated with a hard photon at the current and future hadron colliders. The dependence of the leading order (LO) and NLO EW corrected cross sections on the photon transverse momentum cut are investigated. We also provide the LO and NLO EW corrected distributions of the transverse momentum of final top quark and photon and the invariant mass of top quark pair and top-antitop-photon system. The results show that the NLO EW corrections are significant in high energy regions due to the EW Sudakov effect.

PACS numbers:

* dayu@nju.edu.cn

I. INTRODUCTION

In the standard model (SM), the top quark is a very special particle. Because its mass is much larger than any other SM elementary particles (except Higgs boson), the top quark is speculated to play a special role in electroweak symmetry breaking (EWSB). Since its unique properties have long been believed of potentially carrying important information to solve some of the paramount open questions in particle physics, precise measurements of the cross sections and properties of top quark production channels are significant. With the measurement of the cross section of top quark pair production in association with a hard photon, the strength of the electromagnetic coupling of the top quark and photon can be probed directly.

Experimentally, measurements of the production rate of $t\bar{t}\gamma$ have been performed in $p\bar{p}$ collisions at the Tevatron by the CDF Collaboration at $\sqrt{s} = 1.96$ TeV [1] and in pp collisions at the LHC by the ATLAS Collaboration at $\sqrt{s} = 7$ TeV [2] and by the CMS Collaboration at $\sqrt{s} = 8$ TeV [3]. From the theoretical point of view, the calculation of the cross section of $t\bar{t}\gamma$ production at hadron colliders beyond the leading order (LO) used to be a very challenging problem. The calculation of NLO QCD corrections to the production of $t\bar{t}$ pair and a hard photon at the Tevatron and the LHC have been performed in Refs.[4–6], which has a strong phenomenological motivation due to the large K -factor.

With both the energy and luminosity increment in Run II of the LHC compared with Run I and future hadron colliders whose energy can be up to 100 TeV [7, 8] planned to be built, the need to increase the precision of the perturbative predictions becomes important and urgent. At fixed order, there are two ways [9, 10]: computing either the next-to-next-to-leading order (NNLO) QCD or the NLO electroweak (EW) corrections, which are believed to be comparable numerically. Although the NLO EW correction is normally suppressed by the smallness of the coupling constant α and nominally subdominant with respect to the QCD contributions, the NLO EW correction can become significant in the high-energy domain due to the appearance of Sudakov logarithms [11–13] that result from the virtual exchange of soft or collinear massive weak gauge boson. In this paper, we aim at the NLO EW corrections for the $t\bar{t}\gamma$ production at the LHC and at future higher energy hadron colliders and present the results for the first time.

The rest of the paper is organized as follows: In section II, we provide a general setup of our calculation. In section III, we present the numerical results and discussions for the LO and NLO EW corrected integrated and differential cross sections. Finally, a short summary is given in section IV.

II. CALCULATION SETUP

For the process $pp \rightarrow t\bar{t}\gamma + X$, at tree level the main partonic subprocesses are $gg \rightarrow t\bar{t}\gamma$ and $q\bar{q} \rightarrow t\bar{t}\gamma$, where q denotes the light quarks (u, d, c, s, b) if not otherwise stated. The corresponding representative Feynman diagrams are displayed in Fig.1. We can see that, the tree level amplitudes of the subprocess $gg \rightarrow t\bar{t}\gamma$ can be obtained from the Feynman diagrams in the first line of Fig.1(1-4) which are all at $\mathcal{O}(\alpha_s\alpha^{1/2})$, while for the subprocess $q\bar{q} \rightarrow t\bar{t}\gamma$, the diagrams consist of two types: the gluon-mediated at $\mathcal{O}(\alpha_s\alpha^{1/2})$ depicted in the second line of Fig.1(5-8) and the Z/γ -mediated at $\mathcal{O}(\alpha^{3/2})$ depicted in the third line of Fig.1(9-12). Here, we assume that the CKM matrix is diagonal ¹. Then, the cross section will have different order of α_S and α and can be written as follows:

$$\begin{aligned}\sigma_{tree-level} &= \sigma^{gg}(\alpha_S^2\alpha) + \sigma^{q\bar{q}}(\alpha_S^2\alpha) + \sigma^{q\bar{q}}(\alpha^3) + \sigma^{b\bar{b}}(\alpha_S\alpha^2) \\ &\equiv \sigma_{LO,1}(\alpha_S^2\alpha) + \sigma_{LO,2}(\alpha_S\alpha^2) + \sigma_{LO,3}(\alpha^3)\end{aligned}\quad (1)$$

This equation implicitly defines the leading, second-leading, and third-leading contributions in terms of the order of α_S . At the order of $\alpha_S\alpha^2$, the contributions from the gluon-mediated diagrams interfacing with the Z/γ -mediated ones vanish owing to the color structure for the light quark initial states $q\bar{q}$, while the gluon-mediated diagrams interfacing with the W -exchanged ones survive for $b\bar{b}$ initial state ². The first term $\sigma_{LO,1}(\alpha_S^2\alpha)$ is traditional contribution at LO and labelled as σ_{LO} in this paper.

Analogously, at the one-loop level, i.e., NLO, one has

$$\Delta\sigma_{one-loop-level} \equiv \Delta\sigma_{NLO,1}(\alpha_S^3\alpha) + \Delta\sigma_{NLO,2}(\alpha_S^2\alpha^2) + \Delta\sigma_{LO,3}(\alpha_S\alpha^3) + \Delta\sigma_{LO,4}(\alpha^4)\quad (2)$$

The contributions from the first term $\Delta\sigma_{NLO,1}(\alpha_S^3\alpha)$ consist of the NLO QCD corrections which have been report in Refs.[4, 6]. The second term $\Delta\sigma_{NLO,2}(\alpha_S^2\alpha^2)$ labelled as $\Delta\sigma_{NLO,EW}$ will be calculated for the first time here, since it make up the NLO EW corrections. ³ Then, we define the NLO electroweak corrected cross section as

$$\begin{aligned}\sigma_{NLO,EW} &= \sigma_{LO} + \Delta\sigma_{NLO,EW} \\ &= \sigma_{LO} \times (1 + \delta_{NLO,EW})\end{aligned}\quad (3)$$

¹ For the bottom quark initial state $b\bar{b}$, another type will be exist, i.e., the W -exchanged at $\mathcal{O}(\alpha^{3/2})$, displayed in the last line of Fig.1(13-16).

² When the assumption of diagonal CKM matrix is relaxed, these contributions for $q\bar{q} \rightarrow t\bar{t}\gamma$ subprocess can also be non-zero but are CKM-suppressed.

³ The contributions at $\mathcal{O}(\alpha_S^2\alpha^2)$ can also come from the QCD corrections to $\sigma_{LO,2}(\alpha_S\alpha^2)$, which will be ignored here due to their tininess.

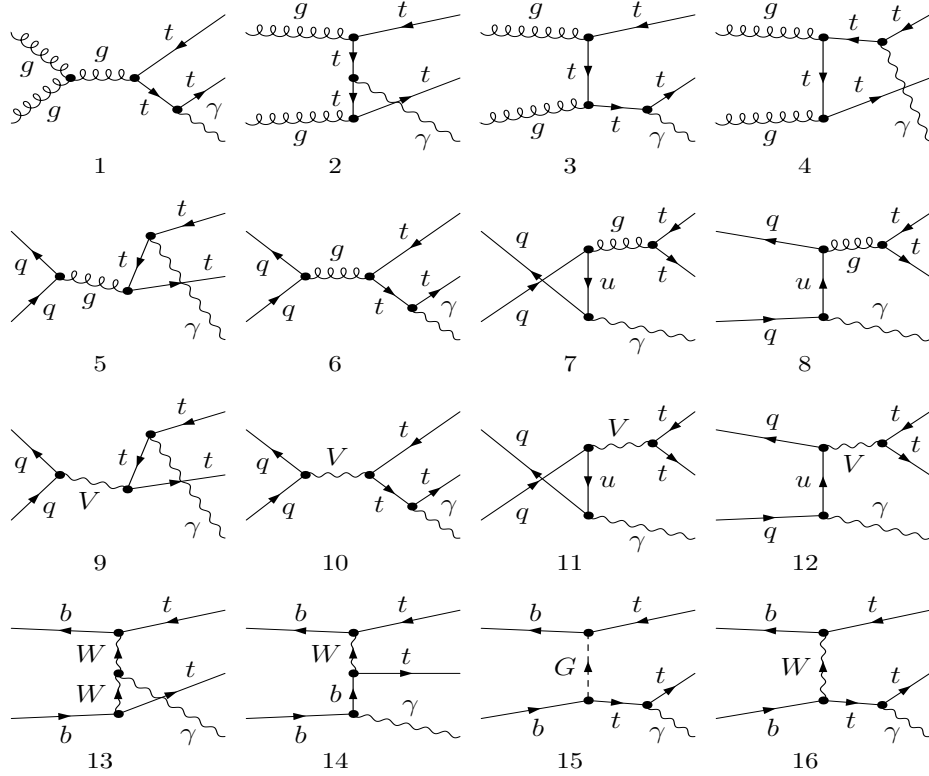


FIG. 1: The representative Feynman diagrams at tree level, where $V = Z, \gamma$.

where $\delta_{NLO,EW} \equiv \frac{\sigma_{NLO,EW} - \sigma_{LO}}{\sigma_{LO}}$ is the corresponding relative NLO EW corrections.

The calculation for the $pp \rightarrow t\bar{t}\gamma + X$ process is performed by using the 't Hooft-Feynman gauge. The parent hadronic process $pp \rightarrow t\bar{t}\gamma + X$ is contributed by $gg \rightarrow t\bar{t}\gamma$ and $q\bar{q} \rightarrow t\bar{t}\gamma$ partonic processes, and the NLO EW corrections decompose two parts: the virtual and real emission correction. In the virtual correction, there exists ultraviolet (UV) and infrared (IR) divergences, which can be isolated by adopting the dimensional regularization (DR) scheme. After performing the renormalization procedure, the UV divergences can be removed through proper counter terms [14, 15] and a UV finite result will be obtained.

In the calculation of the NLO EW corrections to the subprocess $gg \rightarrow t\bar{t}\gamma$, the photonic IR divergences originating from exchange of virtual photon in loop can be cancelled with ones in the real photon emission correction from $gg \rightarrow t\bar{t}\gamma\gamma$ process. In order to extract the IR divergences in the virtual and real corrections, the two cutoff phase space slicing (TCPSS) method [16] is adopted. In addition, the dipole subtraction (DS) method, in which we transfer the dipole formulae in QCD provided in Refs.[17–19] in a straightforward way to the case of dimensionally regularised photon emission, is used to verify the validity of the result.

For the NLO EW corrections at $\mathcal{O}(\alpha_s^2\alpha^2)$ to the subprocess $q\bar{q} \rightarrow t\bar{t}\gamma$, the virtual contribu-

tions consist of two parts: the $\mathcal{O}(\alpha_s\alpha^{1/2})$ gluon-mediated tree-level amplitudes interfering with $\mathcal{O}(\alpha_s\alpha^{3/2})$ one-loop ones which may contain either photonic IR divergences or gluonic IR divergences and the $\mathcal{O}(\alpha^{3/2})$ Z/γ -mediated tree-level amplitudes interfering with $\mathcal{O}(\alpha_s^2\alpha^{1/2})$ one-loop ones which contain gluonic IR divergences. In order to cancel both the photonic and gluonic IR divergences in the virtual contributions, the corresponding real photon emission and real gluon emission corrections should be introduced at the same order of $\alpha_s^2\alpha^2$. The contributions of real photon emission come from the Feynman diagrams at $\mathcal{O}(\alpha_s\alpha)$ of $q\bar{q} \rightarrow t\bar{t}\gamma\gamma$ subprocess, and the real gluon emission corrections contribute by the Feynman diagrams at $\mathcal{O}(\alpha_s^{3/2}\alpha^{1/2})$ interfering with ones at $\mathcal{O}(\alpha_s^{1/2}\alpha^{3/2})$ of $q\bar{q} \rightarrow t\bar{t}\gamma g$ subprocess. Here we find that only the contributions from the interference between the initial and final state gluon radiation diagrams are nonzero owing to the color structure. All the photonic and gluonic IR divergences in the virtual and real emission corrections are extracted by the TCPSS method and the DS method are also applied to check.

The FeynArts-3.7 package [20] is applied to generate the Feynman diagrams automatically and the corresponding amplitudes are algebraically simplified by the FormCalc-7.2 program [21]. In the calculation of one-loop Feynman amplitudes, we adopt the LOOPTOOLS-2.8 package [21] for the numerical calculations of the scalar and tensor integrals, in which the n -point ($n \leq 4$) tensor integrals are reduced to scalar integrals recursively by using Passarino-Veltman algorithm and the 5-point integrals are decomposed into 4-point integrals by using the method of Denner and Dittmaier [22]. In our previous work [23–27], we addressed the numerical instability originating from the small Gram determinant ($\det G$) and scalar one-loop 4-point integrals [28]. In order to solve these instability problems in the numerical calculations, we developed the LOOPTOOLS-2.8 package, which can automatically switch to the quadruple precision codes in the region of small Gram determinants, and checked the results with ones by using ONELOOP package [29] to verify the correctness of our codes.

III. NUMERICAL RESULTS

In our numerical evaluations we take the particles masses as follows:

$$\begin{aligned} M_W &= 80.385 \text{ GeV}, & M_Z &= 91.1876 \text{ GeV}, \\ M_H &= 125 \text{ GeV}, & m_t &= 173.5 \text{ GeV}. \end{aligned} \tag{4}$$

All widths are set equal to zero. Our default EW scheme is the $\alpha(0)$ scheme, where we set:

$$\alpha(0) = 1/137.035999074 \tag{5}$$

$p_T^{\gamma, cut}$ [GeV]		50	100	200	500	1000
σ_{LO}	13 TeV [fb]	851.4(3)	356.1(2)	93.12(4)	4.596(2)	0.14778(4)
	100 TeV [pb]	61.42(2)	30.47(2)	10.616(6)	1.1123(7)	0.10661(7)
$\sigma_{NLO, EW}$	13 TeV [fb]	835.4(4)	348.4(3)	89.92(5)	4.205(3)	0.1259(4)
	100 TeV [pb]	60.04(3)	29.69(3)	10.205(8)	1.0158(9)	0.09068(9)
$\delta_{NLO, EW}$ [%]	13 TeV	-1.9	-2.2	-3.4	-8.5	-14.8
	100 TeV	-2.2	-2.6	-3.9	-8.7	-14.9

TABLE I: The LO and NLO EW corrected integrated cross sections and the corresponding relative NLO EW corrections to the $pp \rightarrow t\bar{t}\gamma + X$ production at the 13 TeV LHC and 100 TeV proton-proton colliders for some typical values of $p_T^{\gamma, cut}$.

We adopt the MSTWlo2008[30] PDFs with the associated $\alpha_S(M_Z)$ for all NLO EW as well as LO predictions, since we are chiefly interested in assessing effects of matrix-element origin. We factorize and absorb initial state photonic collinear singularities into the PDFs by using the DIS factorization scheme. The renormalization (μ_R) and the factorization (μ_F) scales are set to be equal, $\mu_R = \mu_F = m_t$.

In order to exclude the inevitably IR divergence at tree level, we require the final state photon tagged hard with $p_T^\gamma > p_T^{\gamma, cut}$. If additional photon bremsstrahlung is present, any further phase-space cuts will only be applied to the visible photon with highest p_T , while the other is treated inclusively to ensure IR safety.

In table I, we list the LO and NLO EW corrected cross sections and the corresponding relative NLO EW corrections to $t\bar{t}\gamma$ production at the 13 TeV LHC and 100 TeV proton-proton colliders for some typical values of $p_T^{\gamma, cut}$ separately. From this table we find that with the increment of $p_T^{\gamma, cut}$, the NLO EW correction becomes more significant due to the large EW Sudakov logarithms. For $p_T^{\gamma, cut} = 1000$ GeV, the NLO EW corrections are all almost 15% for the 13 TeV LHC and 100 TeV hadron colliders.

In the following, we turn to present results for kinematic distributions of final particles at the 13 TeV LHC with $p_T^{\gamma, cut} = 50$ GeV. The relative NLO EW corrections to the differential cross section $d\sigma/dx$ are defined as $\delta(x) = \left(\frac{d\sigma_{NLO, EW}}{dx} - \frac{\sigma_{LO}}{dx} \right) / \frac{\sigma_{LO}}{dx}$, where x denotes kinematic observable. In the following, the considered observables contain the transverse momentum of the top quark (p_T^t) and the hard photon (p_T^γ) and the invariant mass of $t\bar{t}$ pair ($M_{t\bar{t}}$) and top pair association with a hard photon system ($M_{t\bar{t}\gamma}$).

In Fig.2(a) and (b), we depict the LO and NLO EW corrected distributions for the transverse

momentum of the top quark (p_T^t) and the hard photon (p_T^γ). The Fig.3(a) and (b) present the LO and NLO EW corrected invariant mass distributions of $t - \bar{t}$ ($M_{t\bar{t}}$) and $t - \bar{t} - \gamma$ ($M_{t\bar{t}\gamma}$) system separately. The corresponding relative NLO EW corrections are also shown. We can see that all the relative EW corrections to the considered four observables distributions mostly decrease with the increment of p_T^t , p_T^γ , $M_{t\bar{t}}$ and $M_{t\bar{t}\gamma}$ in the plotted region. The LO p_T^t distributions are enhanced by NLO EW corrections when $p_T^t < 80$ GeV and suppressed in the rest plotted region, while the LO differential cross section of p_T^γ are always suppressed by NLO EW corrections in the whole plotted region. The relative EW corrections to $M_{t\bar{t}}$ and $M_{t\bar{t}\gamma}$ turn to be negative when $M_{t\bar{t}\gamma} \geq 420$ GeV and $M_{t\bar{t}\gamma} \geq 570$ GeV. Due to the Sudakov effect, the absolute size of the NLO EW relative corrections continuously grow up with the increment of p_T^t , p_T^γ , $M_{t\bar{t}}$ and $M_{t\bar{t}\gamma}$ in the large region, particularly which can amount up to -8.0% at $p_T^t = 600$ GeV, -8.6% at $p_T^\gamma = 600$ GeV, -4.5% at $M_{t\bar{t}} = 1000$ GeV and -5.4% at $M_{t\bar{t}\gamma} = 1500$ GeV.

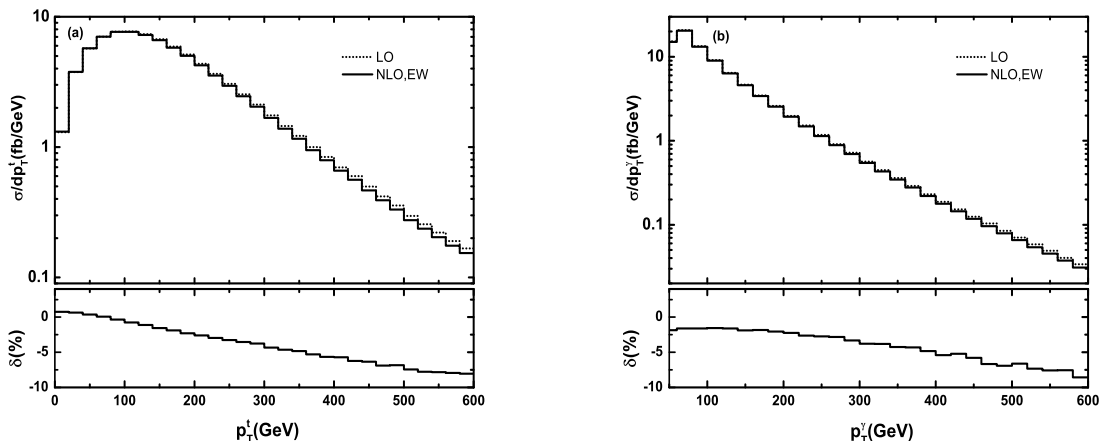


FIG. 2: The LO, NLO EW corrected distributions and the relative NLO EW corrections of $pp \rightarrow t\bar{t}\gamma + X$ process at 13 TeV LHC with $p_T^{\gamma, cut} = 50$ GeV for p_T^t (a) and p_T^γ (b).

IV. SUMMARY

In this work, we present the NLO EW corrections to the $t\bar{t}\gamma$ production at the 13 TeV LHC and future 100 TeV hadron colliders. Our results show that the NLO EW correction is significant in high energy region due to the EW Sudakov effect which can be most probably detected in the LHC experiments and future higher energy hadron colliders. For example, with the photon transverse momentum constraint of $p_T^\gamma > 1$ TeV on the hard photon, the NLO EW corrections to the total cross section of top quark pair production in association with a photon at hadron colliders can

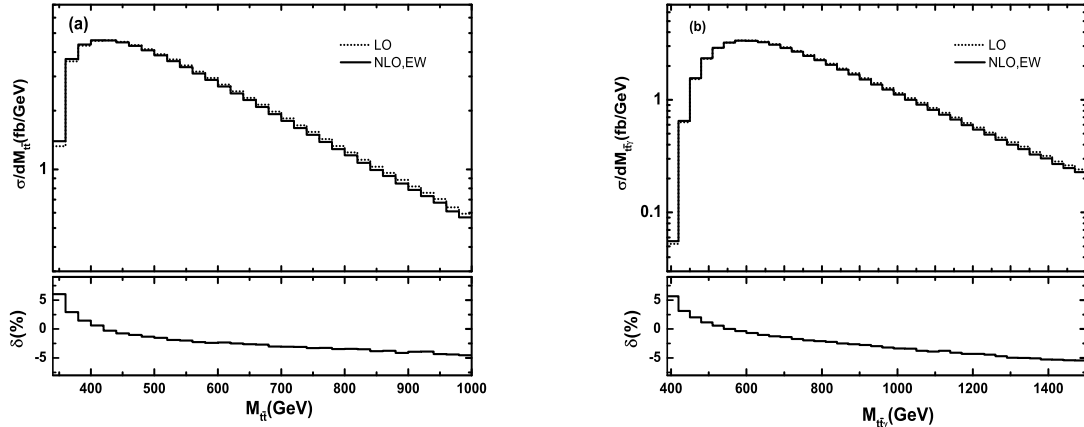


FIG. 3: The LO, NLO EW corrected distributions and the relative NLO EW corrections of $pp \rightarrow t\bar{t}\gamma + X$ process at 13 TeV LHC with $p_T^{\gamma, cut} = 50$ GeV for $M_{t\bar{t}}$ (a) and $M_{t\bar{t}\gamma}$ (b).

reach about -15% with the collide energy $\sqrt{s} = 13$ TeV and 100 TeV. We also investigate the NLO EW effects on the kinematic distributions of p_T^t , p_T^γ , $M_{t\bar{t}}$ and $M_{t\bar{t}\gamma}$, and find that the NLO EW corrections become significant in high energy regions.

Acknowledgements

We would like to thank Zuowei Liu for reading and correcting the grammar and spelling mistakes. This work was supported in part by the National Natural Science Foundation of China (Grant No.11405076, No.11347101, No.11305001, No.11205003), the Applied Basic Research Programs of Yunan Provincial Science and Technology Department (Grant No.2016FB008), and the Startup Foundation for Doctors of Kunming University of Science and Technology (No.KKSY201356060).

-
- [1] T. Aaltonen *et al.* [CDF Collaboration], Phys. Rev. D **84** (2011) 031104 doi:10.1103/PhysRevD.84.031104 [arXiv:1106.3970 [hep-ex]].
 - [2] G. Aad *et al.* [ATLAS Collaboration], Phys. Rev. D **91** (2015) no.7, 072007 doi:10.1103/PhysRevD.91.072007 [arXiv:1502.00586 [hep-ex]].
 - [3] CMS Collaboration [CMS Collaboration], CMS-PAS-TOP-14-008.
 - [4] P. F. Duan, W. G. Ma, R. Y. Zhang, L. Han, L. Guo and S. M. Wang, Phys. Rev. D **80** (2009) 014022. doi:10.1103/PhysRevD.80.014022

- [5] D. Peng-Fei, Z. Ren-You, M. Wen-Gan, H. Liang, G. Lei and W. Shao-Ming, *Chin. Phys. Lett.* **28** (2011) 111401 doi:10.1088/0256-307X/28/11/111401 [arXiv:1110.2315 [hep-ph]].
- [6] K. Melnikov, M. Schulze and A. Scharf, *Phys. Rev. D* **83** (2011) 074013 doi:10.1103/PhysRevD.83.074013 [arXiv:1102.1967 [hep-ph]].
- [7] M. Benedikt, “FCC study overview and status”, talk at the FCC week 2016, Rome, 11-15 April 2016, <http://indico.cern.ch/event/438866/contributions/1085016/>.
- [8] CEPC project website. <http://cepc.ihep.ac.cn>.
- [9] J. R. Andersen *et al.*, arXiv:1405.1067 [hep-ph].
- [10] J. R. Andersen *et al.*, arXiv:1605.04692 [hep-ph].
- [11] V. V. Sudakov, *Sov. Phys. JETP* **3** (1956) 65 [*Zh. Eksp. Teor. Fiz.* **30** (1956) 87].
- [12] V. S. Fadin, L. N. Lipatov, A. D. Martin and M. Melles, *Phys. Rev. D* **61** (2000) 094002 doi:10.1103/PhysRevD.61.094002 [hep-ph/9910338].
- [13] P. Ciafaloni and D. Comelli, *Phys. Lett. B* **446** (1999) 278 doi:10.1016/S0370-2693(98)01541-X [hep-ph/9809321].
- [14] D. A. Ross and J. C. Taylor, *Nucl. Phys. B* **51** (1973) 125 Erratum: [*Nucl. Phys. B* **58** (1973) 643]. doi:10.1016/0550-3213(73)90608-1, 10.1016/0550-3213(73)90505-1
- [15] A. Denner, *Fortsch. Phys.* **41** (1993) 307 doi:10.1002/prop.2190410402 [arXiv:0709.1075 [hep-ph]].
- [16] B. W. Harris and J. F. Owens, *Phys. Rev. D* **65** (2002) 094032 doi:10.1103/PhysRevD.65.094032 [hep-ph/0102128].
- [17] S. Catani and M. H. Seymour, *Phys. Lett. B* **378** (1996) 287 doi:10.1016/0370-2693(96)00425-X [hep-ph/9602277].
- [18] S. Catani and M. H. Seymour, *Nucl. Phys. B* **485** (1997) 291 Erratum: [*Nucl. Phys. B* **510** (1998) 503] doi:10.1016/S0550-3213(96)00589-5, 10.1016/S0550-3213(98)81022-5 [hep-ph/9605323].
- [19] S. Catani, S. Dittmaier, M. H. Seymour and Z. Trocsanyi, *Nucl. Phys. B* **627** (2002) 189 doi:10.1016/S0550-3213(02)00098-6 [hep-ph/0201036].
- [20] T. Hahn, *Comput. Phys. Commun.* **140** (2001) 418 doi:10.1016/S0010-4655(01)00290-9 [hep-ph/0012260].
- [21] T. Hahn and M. Perez-Victoria, *Comput. Phys. Commun.* **118** (1999) 153 doi:10.1016/S0010-4655(98)00173-8 [hep-ph/9807565].
- [22] A. Denner and S. Dittmaier, *Nucl. Phys. B* **658** (2003) 175 doi:10.1016/S0550-3213(03)00184-6 [hep-ph/0212259].
- [23] Z. Yu, G. Lei, M. Wen-Gan, Z. Ren-You, C. Chong and L. Xiao-Zhou, *Eur. Phys. J. C* **74** (2014) no.1, 2739 doi:10.1140/epjc/s10052-014-2739-0 [arXiv:1311.7240 [hep-ph]].
- [24] C. Chen, W. G. Ma, R. Y. Zhang, Y. Zhang, L. W. Chen and L. Guo, *Eur. Phys. J. C* **74** (2014) no.11, 3166 doi:10.1140/epjc/s10052-014-3166-y [arXiv:1409.4900 [hep-ph]].
- [25] Y. Zhang, W. G. Ma, R. Y. Zhang, C. Chen and L. Guo, *Phys. Lett. B* **738** (2014) 1 doi:10.1016/j.physletb.2014.09.022 [arXiv:1407.1110 [hep-ph]].

- [26] Y. Zhang, P. F. Duan, W. G. Ma, R. Y. Zhang and C. Chen, *Eur. Phys. J. C* **76** (2016) no.2, 76
doi:10.1140/epjc/s10052-016-3919-x [arXiv:1512.01879 [hep-ph]].
- [27] Y. Zhang, W. H. Li, P. F. Duan, M. Song and G. Li, *Phys. Lett. B* **758** (2016) 42
doi:10.1016/j.physletb.2016.04.054 [arXiv:1604.07921 [hep-ph]].
- [28] F. Boudjema, L. D. Ninh, S. Hao and M. M. Weber, *Phys. Rev. D* **81** (2010) 073007
doi:10.1103/PhysRevD.81.073007 [arXiv:0912.4234 [hep-ph]].
- [29] A. van Hameren, C. G. Papadopoulos and R. Pittau, *JHEP* **0909** (2009) 106 doi:10.1088/1126-6708/2009/09/106 [arXiv:0903.4665 [hep-ph]].
- [30] A. D. Martin, W. J. Stirling, R. S. Thorne and G. Watt, *Eur. Phys. J. C* **63** (2009) 189
doi:10.1140/epjc/s10052-009-1072-5 [arXiv:0901.0002 [hep-ph]].